



THE UNIVERSITY *of* EDINBURGH

Edinburgh Research Explorer

## Chirality in isotropic linear gradient elasticity

**Citation for published version:**

Papanicolopoulos, S-A 2011, 'Chirality in isotropic linear gradient elasticity', *International Journal of Solids and Structures*, vol. 48, no. 5, pp. 745-752. <https://doi.org/10.1016/j.ijsolstr.2010.11.007>

**Digital Object Identifier (DOI):**

[10.1016/j.ijsolstr.2010.11.007](https://doi.org/10.1016/j.ijsolstr.2010.11.007)

**Link:**

[Link to publication record in Edinburgh Research Explorer](#)

**Document Version:**

Peer reviewed version

**Published In:**

International Journal of Solids and Structures

**General rights**

Copyright for the publications made accessible via the Edinburgh Research Explorer is retained by the author(s) and / or other copyright owners and it is a condition of accessing these publications that users recognise and abide by the legal requirements associated with these rights.

**Take down policy**

The University of Edinburgh has made every reasonable effort to ensure that Edinburgh Research Explorer content complies with UK legislation. If you believe that the public display of this file breaches copyright please contact [openaccess@ed.ac.uk](mailto:openaccess@ed.ac.uk) providing details, and we will remove access to the work immediately and investigate your claim.





# Chirality in isotropic linear gradient elasticity

S.-A. Papanicolopoulos<sup>a,\*</sup>

<sup>a</sup>*Department of Mechanics, National Technical University of Athens, Zografou 157 73, Greece*

---

## Abstract

Chirality is, generally speaking, the property of an object that can be classified as left- or right-handed. Though it plays an important role in many branches of science, chirality is encountered less often in continuum mechanics, so most classical material models do not account for it. In the context of elasticity, for example, classical elasticity is not chiral, leading different authors to use Cosserat elasticity to allow modelling of chiral behaviour.

Gradient elasticity can also model chiral behaviour, however this has received much less attention than its Cosserat counterpart. This paper shows how in the case of isotropic linear gradient elasticity a single additional parameter can be introduced that describes chiral behaviour. This additional parameter, directly linked to three-dimensional deformation, can be either negative or positive, with its sign indicating a discrimination between the two opposite directions of torsion. Two simple examples are presented to show the practical effects of the chiral behaviour.

**Keywords:** chirality, microstructure, gradient elasticity, isotropy, torsion

---

## 1. Introduction

The term “chirality” was introduced by [Lord Kelvin \(1904, p. 619\)](#), who gave the following definition:

I call any geometrical figure, or group of points, *chiral*, and say that it has chirality if its image in a plane mirror, ideally realized, cannot be brought

---

\*Corresponding author. Tel.: +30 210 772 1373; fax: +30 210 772 1302.  
Email address: stefanos@mechan.ntua.gr (S.-A. Papanicolopoulos)

to coincide with itself. Two equal and similar right hands are homochirally similar. Equal and similar right and left hands are heterochirally similar [...] Any chiral object and its image in a plane mirror are heterochirally similar.

Chirality is a concept encountered in different branches of mathematics and physics, in biology and most of all in chemistry, where it is the subject of the journals *Chirality* and *Tetrahedron: Asymmetry*. A detailed description of molecular chirality is given by [Mislow \(1999\)](#), while [Cintas \(2007\)](#) provides a history of both the concept of chirality and the term itself, again focusing on chemistry.

In continuum mechanics, a chiral material (also known as non-centrosymmetric, acentric, or hemitropic) is a material whose behaviour is not invariant with respect to inversion (that is, to change of sign of all coordinates). For an overview of chirality in mechanics, see for example [Lakes \(2001\)](#) and [Natroshvili and Stratis \(2006\)](#) and the references contained therein. It should however be noted that chirality is often ignored in mechanics, since many materials do not exhibit it and, conversely, many common material models, including the classical theory of linear elasticity, cannot describe it (see however the discussion of [Fraldi and Cowin \(2002\)](#) concerning chiral anisotropic linear elasticity).

It is therefore common to use Cosserat (or micropolar) elasticity ([Cosserat and Cosserat, 1909](#); [Eringen, 1966](#)) to introduce chirality in the context of elasticity (see [Lakes and Benedict, 1982](#); [Lakes, 2001](#); [Natroshvili and Stratis, 2006](#), and references therein). In isotropic linear Cosserat elasticity, chirality introduces three additional parameters for a total of nine material parameters. The importance of such models is that they can reproduce microstructural effects due to the chirality of the microstructure, mainly in engineered or biological materials.

Gradient elasticity ([Toupin, 1962](#); [Mindlin, 1964](#); [Mindlin and Eshel, 1968](#)) can also describe chiral behaviour, yet this aspect has seen much less interest than chiral Cosserat elasticity. [Toupin \(1962\)](#) introduces a rank-five *rotary tensor* related to wave polarisation, a result later used in other works discussing acoustic activity. [Maranganti and Sharma \(2007\)](#) also consider non-centrosymmetric gradient-elasticity and its rela-

tion to a fifth-order tensor in the context of wave propagation. A different kind of chirality, related to a sixth-order tensor, is given by [Auffray et al. \(2009\)](#) for *bi-dimensional* anisotropic gradient elasticity. There has been however no general presentation of the concept of chirality in three-dimensional gradient elasticity and its effects for the static, mechanical behaviour.

This paper presents the case of isotropic linear gradient elasticity, showing how chirality is present in its general formulation unless, as done by [Mindlin \(1964\)](#), centrosymmetric behaviour is explicitly imposed. An important property of the resulting model is that chiral behaviour is controlled by a single material parameter, in contrast to the three additional material parameters required in Cosserat elasticity. This material parameter can be either positive or negative, but its absolute value is bounded by the requirement for positive definiteness of the potential energy density.

A second interesting property of the model is that the chiral behaviour is related to the gradient of the rotation and is therefore directly linked to the presence of torsion. This makes it necessary to consider problems of three-dimensional deformation. Two such problems, the torsion of a hollow cylinder and the mode III crack, are presented in this paper.

Recently, gradient elasticity has been proposed to model the behaviour of carbon nanotubes ([Zhang et al., 2004](#); [Wang and Hu, 2005](#); [Wang and Wang, 2007](#))<sup>1</sup>. Due to their structure, carbon nanotubes may also exhibit geometrical chirality, which affects their mechanical behaviour (see e.g. [Duan et al., 2007](#); [Zhang et al., 2010](#)). It is therefore conceivable that the chirality of the gradient-elastic model, which is presented in this paper, can be related to the geometric chirality of the nanotube and its effect on the mechanical behaviour.

The structure of the paper is as follows: the necessary concepts concerning isotropic tensors and pseudo-tensors are presented in section 2. Section 3 presents the main concepts of linear gradient elasticity used in this paper, as well as the restriction to the isotropic case. In comparison to the usual, centrosymmetric case, an additional mate-

---

<sup>1</sup>It should be noted that these references use the term “non-local elasticity”, however the actual models used are strain gradient models.

rial parameter is introduced, that is shown in section 4 to introduce chiral behaviour. Section 5 gives the stress-strain relations in tensor form but also in matrix form, the latter providing a clearer picture of the way the stress-strain relation is modified by the introduction of chirality. As a simple example, section 6 shows the chiral behaviour of a cylinder under torsion, giving both an analytical and a numerical solution. A second example, the mode III crack, is also solved numerically. Finally, section 7 presents the main conclusions.

## 2. Isotropic tensors

This section presents briefly the properties of isotropic tensors and pseudo-tensors that will be used in this paper. A more detailed description of the relevant theory can be found in books on tensor algebra (e.g. [Borisenko and Tarapov, 1979](#); [Temple, 2004](#)). To avoid confusion, a clear distinction is made in this paper between tensors and pseudo-tensors by using the term “tensor” only with its usual meaning (i.e. what is sometimes called a polar tensor) while never using it to refer to pseudo-tensors. Indicial notation is used, with indices  $i, j, \dots, p, q$  ranging from 1 to 3 and repeated indices indicating summation. Only Cartesian (pseudo-) tensors are considered, so no distinction is made between covariant and contravariant components.

An isotropic tensor is a tensor that is invariant under rotation. All rank-zero tensors (i.e. scalars) are isotropic, while there are no isotropic rank-one tensors (i.e. vectors). Similarly, isotropic pseudo-tensors are invariant under rotation, all pseudo-scalars are isotropic but there are no isotropic pseudo-vectors.

The only isotropic rank-two tensor is the Kronecker delta  $\delta_{ij}$  (and its multiples). The product of two isotropic tensors is also an isotropic tensor; indeed there are only three linearly independent isotropic tensors of rank four, which can be written as products of two Kronecker deltas. The generic form of an isotropic rank-four tensor is therefore

$$c_{ijkl} = c_1 \delta_{ij} \delta_{kl} + c_2 \delta_{ik} \delta_{jl} + c_3 \delta_{il} \delta_{jk} \quad (1)$$

Similarly, there are fifteen linearly independent rank-six tensors, which can be written as products of three Kronecker deltas, so the generic form of an isotropic rank-six

tensor is

$$\begin{aligned}
a_{ijklmn} = & a_1 \delta_{ij} \delta_{kl} \delta_{mn} + a_2 \delta_{ij} \delta_{km} \delta_{ln} + a_3 \delta_{ij} \delta_{kn} \delta_{lm} \\
& + a_4 \delta_{ik} \delta_{jl} \delta_{mn} + a_5 \delta_{ik} \delta_{jm} \delta_{ln} + a_6 \delta_{ik} \delta_{jn} \delta_{lm} \\
& + a_7 \delta_{il} \delta_{jk} \delta_{mn} + a_8 \delta_{im} \delta_{jk} \delta_{ln} + a_9 \delta_{in} \delta_{jk} \delta_{lm} \\
& + a_{10} \delta_{il} \delta_{jm} \delta_{kn} + a_{11} \delta_{im} \delta_{jl} \delta_{kn} + a_{12} \delta_{in} \delta_{jl} \delta_{km} \\
& + a_{13} \delta_{il} \delta_{jn} \delta_{km} + a_{14} \delta_{im} \delta_{jn} \delta_{kl} + a_{15} \delta_{in} \delta_{jm} \delta_{kl}
\end{aligned} \tag{2}$$

The only isotropic rank-three pseudo-tensor is the permutation pseudo-tensor  $e_{ijk}$  (and its multiples). Since  $e_{ijk}$  is an isotropic pseudo-tensor, then its product with the isotropic tensor  $\delta_{lm}$  is also an isotropic pseudo-tensor. Ten such outer products can be formed, since permutation of the indices of  $e_{ijk}$  at most changes the sign while permutation of the indices of  $\delta_{lm}$  does not change anything. These can be written as

$$\begin{aligned}
& \{e_{ijk} \delta_{lm}, e_{ilk} \delta_{jm}, e_{imk} \delta_{jl}, e_{jlk} \delta_{im}, e_{jmk} \delta_{il}, \\
& e_{lmk} \delta_{ij}, e_{ijl} \delta_{mk}, e_{ijm} \delta_{lk}, e_{ilm} \delta_{jk}, e_{jlm} \delta_{ik}\}
\end{aligned} \tag{3}$$

Boyle and Matthews (1971) show that any group of four products in equation (3) where the  $\delta$  have a common index (e.g. the last four products all have  $k$  as index of  $\delta$ ) can be written as a linear combination of the remaining six products. There are therefore only six linearly independent products in (3), so that the generic form of the isotropic rank-five pseudo-tensor can be written as

$$\begin{aligned}
f_{ijklm} = & f_1 e_{ijk} \delta_{lm} + f_2 e_{ilk} \delta_{jm} + f_3 e_{imk} \delta_{jl} \\
& + f_4 e_{jlk} \delta_{im} + f_5 e_{jmk} \delta_{il} + f_6 e_{lmk} \delta_{ij}
\end{aligned} \tag{4}$$

where  $f_1, \dots, f_6$  are arbitrary coefficients. Note that if all the coefficients  $f_1, \dots, f_6$  in equation (4) are pseudo-scalars instead of scalars, then  $f_{ijklm}$  is an isotropic rank-five tensor.

### 3. Gradient elasticity

#### 3.1. Linear gradient elasticity

A detailed description of gradient elasticity and the derivation of its equations is given by Mindlin (1964) and Mindlin and Eshel (1968). This section therefore only

presents the basic points needed in the present paper, for the static, small strain case in Cartesian coordinates. Three different forms of gradient elasticity are usually formulated which are equivalent, so it is generally only necessary to consider one of them. Both form II and form III will be used here, however, to better emphasise some aspects of the introduction of chiral behaviour.

Consider a body subject to a displacement field  $u_i$ . In form II of gradient elasticity the kinematic quantities are the strain  $\epsilon_{ij}$  and the strain gradient  $\hat{\kappa}_{ijk}$  defined as

$$\epsilon_{ij} = \frac{1}{2}(u_{i,j} + u_{j,i}), \quad \hat{\kappa}_{ijk} = \epsilon_{jk,i} \quad (5)$$

The potential energy density function is in this case

$$\hat{W} = \hat{W}(\epsilon_{ij}, \hat{\kappa}_{ijk}) \quad (6)$$

and its variation introduces the stresses  $\tau_{ij} = \partial \hat{W} / \partial \epsilon_{ij}$  and double stresses  $\hat{\mu}_{ijk} = \partial \hat{W} / \partial \hat{\kappa}_{ijk}$  which are energy conjugate to the strains and strain gradients respectively.

For form III, the kinematic quantities are the strain  $\epsilon_{ij}$ , the gradient of the rotation  $\bar{\kappa}_{ij}$  and the fully symmetric part of the second gradient of the displacement  $\bar{\bar{\kappa}}_{ijk}$ , defined as

$$\begin{aligned} \epsilon_{ij} &= \frac{1}{2}(u_{i,j} + u_{j,i}), & \bar{\kappa}_{ij} &= \frac{1}{2}e_{jlk}u_{k,li}, \\ \bar{\bar{\kappa}}_{ijk} &= \frac{1}{3}(u_{k,ij} + u_{i,jk} + u_{j,ki}) \end{aligned} \quad (7)$$

The potential energy density function is expressed as

$$W = \bar{W}(\epsilon_{ij}, \bar{\kappa}_{ij}, \bar{\bar{\kappa}}_{ijk}) \quad (8)$$

and its variation introduces the static quantities  $\tau_{ij}$ ,  $\bar{\mu}_{ij}$  and  $\bar{\bar{\mu}}_{ijk}$ , energy conjugate to  $\epsilon_{ij}$ ,  $\bar{\kappa}_{ij}$  and  $\bar{\bar{\kappa}}_{ijk}$  respectively.

In linear gradient elasticity,  $\hat{W}$  and  $\bar{W}$  are given by the general forms

$$\hat{W} = \frac{1}{2}\hat{c}_{ijkl}\epsilon_{ij}\epsilon_{kl} + \hat{f}_{ijklm}\hat{\kappa}_{ijk}\epsilon_{lm} + \frac{1}{2}\hat{a}_{ijklmn}\hat{\kappa}_{ijk}\hat{\kappa}_{lmn} \quad (9)$$

$$\begin{aligned} \bar{W} &= \frac{1}{2}\bar{c}_{ijkl}\epsilon_{ij}\epsilon_{kl} + \frac{1}{2}\bar{d}_{ijkl}\bar{\kappa}_{ij}\bar{\kappa}_{kl} + \frac{1}{2}\bar{a}_{ijklmn}\bar{\bar{\kappa}}_{ijk}\bar{\bar{\kappa}}_{lmn} \\ &\quad + \bar{b}_{ijkl}\epsilon_{ij}\bar{\kappa}_{kl} + \bar{f}_{ijklm}\bar{\kappa}_{ij}\bar{\bar{\kappa}}_{klm} + \bar{g}_{ijklm}\epsilon_{ij}\bar{\bar{\kappa}}_{klm} \end{aligned} \quad (10)$$

where the tensors  $\hat{c}_{ijkl}$ ,  $\hat{f}_{ijklm}$ ,  $\hat{a}_{ijklmn}$  and  $\bar{c}_{ijkl}$ ,  $\bar{d}_{ijkl}$ ,  $\bar{a}_{ijklmn}$ ,  $\bar{b}_{ijkl}$ ,  $\bar{f}_{ijklm}$ ,  $\bar{g}_{ijklm}$  form two alternative sets of material parameters. Taking into account various symmetry requirements for these tensors, the number of independent material parameters is respectively 21, 108, 171 for  $\hat{c}_{ijkl}$ ,  $\hat{f}_{ijklm}$ ,  $\hat{a}_{ijklmn}$  and 21, 36, 55, 48, 80, 60 for  $\bar{c}_{ijkl}$ ,  $\bar{d}_{ijkl}$ ,  $\bar{a}_{ijklmn}$ ,  $\bar{b}_{ijkl}$ ,  $\bar{f}_{ijklm}$ ,  $\bar{g}_{ijklm}$ , for a total of 300 independent material parameters in either case.

Considering form II, [Giannakopoulos et al. \(2006\)](#) prove the reciprocity theorem for linear gradient elasticity for the case where  $\hat{f}_{ijklm} = 0$ , while [Georgiadis and Grentzelou \(2006\)](#) give a similar result for form I. The proof for the case  $\hat{f}_{ijklm} \neq 0$  is given by [Papanicolopoulos \(2008\)](#) and independently by [Agiarofitou and Lazar \(2009\)](#), showing that there is no reason to consider *a priori* the term  $\hat{f}_{ijklm}$  as introducing a different material behaviour.

### 3.2. Isotropic linear gradient elasticity

To obtain a form II isotropic linear gradient elasticity, the  $\hat{c}_{ijkl}$ ,  $\hat{f}_{ijklm}$  and  $\hat{a}_{ijklmn}$  tensors must all be isotropic. Using the general forms of isotropic tensors (1) and (2) and taking into account the symmetries of  $\epsilon_{ij}$  and  $\hat{k}_{ijk}$  we obtain

$$\hat{c}_{ijkl}\epsilon_{ij}\epsilon_{kl} = \lambda\epsilon_{ii}\epsilon_{jj} + 2\mu\epsilon_{ij}\epsilon_{ij} \quad (11)$$

$$\begin{aligned} \hat{a}_{ijklmn}\hat{k}_{ijk}\hat{k}_{lmn} &= 2(\hat{a}_1\hat{k}_{iik}\hat{k}_{kjj} + \hat{a}_2\hat{k}_{kii}\hat{k}_{kjj} + \hat{a}_3\hat{k}_{iik}\hat{k}_{jjk} \\ &\quad + \hat{a}_4\hat{k}_{ijk}\hat{k}_{ijk} + \hat{a}_5\hat{k}_{ijk}\hat{k}_{jik}) \end{aligned} \quad (12)$$

Considering  $\hat{f}_{ijklm}$  as an isotropic rank-five tensor, as discussed in section 2, and taking again into account the symmetries of  $\epsilon_{ij}$  and  $\hat{k}_{ijk}$  we obtain

$$\begin{aligned} \hat{f}_{ijklm}\hat{k}_{ijk}\epsilon_{lm} &= (f_1e_{ijk}\delta_{lm} + f_2e_{ilk}\delta_{jm} + f_3e_{imk}\delta_{jl} \\ &\quad + f_4e_{jlk}\delta_{im} + f_5e_{jmk}\delta_{il} + f_6e_{lmk}\delta_{ij})\hat{k}_{ijk}\epsilon_{lm} \\ &= (f_2 + f_3)e_{ilk}\hat{k}_{ijk}\epsilon_{jl} \\ &= -(f_2 + f_3)e_{ikl}\hat{k}_{ijk}\epsilon_{jl} \\ &= 2\hat{f}e_{ikl}\hat{k}_{ijk}\epsilon_{jl} \end{aligned} \quad (13)$$

where we have set  $\hat{f} = -(f_2 + f_3)/2$ . Since  $f_1, \dots, f_6$  are arbitrary pseudo-scalar coefficients,  $\hat{f}$  is also a pseudo-scalar, whose meaning will be considered later.



The potential energy density is then rewritten as

$$\begin{aligned}\hat{W} = & \frac{1}{2}\lambda\epsilon_{ii}\epsilon_{jj} + \mu\epsilon_{ij}\epsilon_{ij} + \hat{a}_1\hat{k}_{iik}\hat{k}_{kjj} + \hat{a}_2\hat{k}_{kii}\hat{k}_{kjj} + \hat{a}_3\hat{k}_{iik}\hat{k}_{jjk} \\ & + \hat{a}_4\hat{k}_{ijk}\hat{k}_{ijk} + \hat{a}_5\hat{k}_{ijk}\hat{k}_{jik} + 2\hat{f}e_{ikl}\hat{k}_{ijk}\epsilon_{jl}\end{aligned}\quad (14)$$

Similar calculations for form III, taking into account that  $\epsilon_{ij}$  is symmetric,  $\bar{k}_{ij}$  is traceless ( $\bar{k}_{ii} = 0$ ) and  $\bar{k}_{ijk}$  is fully symmetric, give the value of  $\bar{W}$  for the isotropic case

$$\begin{aligned}\bar{W} = & \frac{1}{2}\lambda\epsilon_{ii}\epsilon_{jj} + \mu\epsilon_{ij}\epsilon_{ij} + 2\bar{d}_1\bar{k}_{ij}\bar{k}_{ij} + 2\bar{d}_2\bar{k}_{ij}\bar{k}_{ji} \\ & + \frac{3}{2}\bar{a}_1\bar{k}_{iik}\bar{k}_{jjk} + \bar{a}_2\bar{k}_{ijk}\bar{k}_{ijk} + \bar{f}e_{ijk}\bar{k}_{ij}\bar{k}_{kll} + 2\bar{b}\epsilon_{ij}\bar{k}_{ij}\end{aligned}\quad (15)$$

where the term  $\bar{b}$  is derived from the term  $\bar{b}_{ijkl}$  in equation (10), by computations similar to those in equation (13) that derive  $\hat{f}$  from  $\hat{f}_{ijklm}$ .

In equations (14) and (15), the last term is an additional one which does not appear in the usual, non-chiral formulation. This term introduces one additional material parameter which, as will be seen in section 4, introduces chirality in the material behaviour. Comparing the last terms in equations (14) and (15) and noting that  $e_{ikl}\hat{k}_{ijk}\epsilon_{jl} = \epsilon_{ij}\bar{k}_{ij}$  we obtain the relation

$$\bar{b} = \hat{f} \quad (16)$$

Limits on the possible values of  $\bar{b}$  (and  $\hat{f}$ ) are imposed by the requirement for positive definiteness of  $\bar{W}$ . Consider the following decomposition of the kinematic quantities of Form III:

$$\epsilon_{ij} = \epsilon_{ij}^s + \epsilon_{ij}^d, \quad \bar{k}_{ij} = \bar{k}_{ij}^d + \bar{k}_{ij}^a, \quad \bar{k}_{ijk} = \bar{k}_{ijk}^s + \bar{k}_{ijk}^d \quad (17)$$

where

$$\begin{aligned}\epsilon_{ij}^s &= \frac{1}{3}\epsilon_{pp}\delta_{ij}, \quad \epsilon_{ij}^d = \epsilon_{ij} - \epsilon_{ij}^s, \quad \bar{k}_{ij}^d = \bar{k}_{(ij)}, \quad \bar{k}_{ij}^a = \bar{k}_{[ij]} \\ \bar{k}_{ijk}^s &= \frac{1}{5}(\bar{k}_{ill}\delta_{jk} + \bar{k}_{jll}\delta_{ik} + \bar{k}_{kll}\delta_{ij}), \quad \bar{k}_{ijk}^d = \bar{k}_{ijk} - \bar{k}_{ijk}^s\end{aligned}\quad (18)$$

Substituting into equation (15) yields

$$\begin{aligned}\bar{W} = & \frac{1}{2}(3\lambda + 2\mu)\epsilon_{ij}^s\epsilon_{ij}^s + \mu\epsilon_{ij}^d\epsilon_{ij}^d + 2(\bar{d}_1 + \bar{d}_2)\bar{k}_{ij}^d\bar{k}_{ij}^d \\ & + 2(\bar{d}_1 - \bar{d}_2)\bar{k}_{ij}^a\bar{k}_{ij}^a + \frac{1}{2}(5\bar{a}_1 + 2\bar{a}_2)\bar{k}_{ijk}^s\bar{k}_{ijk}^s \\ & + \bar{a}_2\bar{k}_{ijk}^d\bar{k}_{ijk}^d + \bar{f}e_{ijk}\bar{k}_{ij}^a\bar{k}_{kll}^s + 2\bar{b}\epsilon_{ij}^d\bar{k}_{ij}^d\end{aligned}\quad (19)$$

This equation yields the necessary and sufficient conditions for positive definiteness of  $\bar{W}$ . Besides the seven conditions given by [Mindlin and Eshel \(1968\)](#)

$$\begin{aligned} \mu &> 0, & 3\lambda + 2\mu &> 0, & \bar{d}_1 + \bar{d}_2 &> 0, \\ \bar{a}_2 &> 0, & 5\bar{a}_1 + 2\bar{a}_2 &> 0, & \bar{d}_1 - \bar{d}_2 &> 0, \\ 5\bar{f}^2 &< 6(\bar{d}_1 - \bar{d}_2)(5\bar{a}_1 + 2\bar{a}_2) \end{aligned} \quad (20)$$

the second, third and eighth terms of (19) yield the additional condition

$$\bar{b}^2 < 2\mu(\bar{d}_1 + \bar{d}_2) \quad (21)$$

or, for form II,

$$3\hat{f}^2 < \mu(2\hat{a}_4 - \hat{a}_5) \quad (22)$$

### 3.3. Comparison with the “gradient elasticity with surface energy” model

Based on early work by [Casal \(1961\)](#), [Vardoulakis et al. \(1996\)](#) proposed a model of anisotropic linear gradient elasticity with surface energy. In its most general form, this model is a linear gradient elasticity where, using a form II formulation,  $\hat{f}_{ijklm} \neq 0$  and  $\hat{f}_{ijklm} = \hat{f}_{ilmjk}$ .

Both the model introduced in this paper and the surface-energy model are linear gradient elastic models whose potential energy density function includes products of first and second derivatives of the displacements (in form II this means  $\hat{f}_{ijklm} \neq 0$ ). The two models, however, are clearly *not related*: the model introduced in this paper is isotropic, does not have surface energy and (as will be shown in section 4) exhibits chiral behaviour.

Considering the term of the potential energy density in equation (9) that depends on  $\hat{f}_{ijklm}$ , we calculate

$$\begin{aligned} \hat{W}^f &\equiv \hat{f}_{ijklm} \hat{\kappa}_{ijk} \epsilon_{lm} \\ &= \frac{1}{2} \left( (\hat{f}_{ijklm} \epsilon_{jk} \epsilon_{lm})_{,i} - \hat{f}_{ijklm,i} \epsilon_{jk} \epsilon_{lm} \right. \\ &\quad \left. - (\hat{f}_{ijklm} - \hat{f}_{ilmjk}) \epsilon_{jk} \epsilon_{lm,i} \right) \end{aligned} \quad (23)$$

The potential energy in a volume  $V$  bounded by a surface  $S$  with unit normal vector  $n_i$  is then given, using the divergence theorem, by

$$\begin{aligned} \hat{\mathcal{W}}^f \equiv \int_V \hat{W}^f dV &= \frac{1}{2} \int_S n_i \hat{f}_{ijklm} \epsilon_{jk} \epsilon_{lm} dS \\ &- \frac{1}{2} \int_V \left( \hat{f}_{ijklm,i} \epsilon_{jk} \epsilon_{lm} + (\hat{f}_{ijklm} - \hat{f}_{ilmjk}) \epsilon_{jk} \epsilon_{lm,i} \right) dV \end{aligned} \quad (24)$$

Equation (24) shows that, assuming  $\hat{f}_{ijklm}$  is non-zero and spatially constant, the symmetry  $\hat{f}_{ijklm} = \hat{f}_{ilmjk}$  is enough to ensure that  $\hat{f}_{ijklm}$  only contributes to the surface energy of the material. From equation (13) the form of  $\hat{f}_{ijklm}$  for the present model can be written, imposing the necessary symmetries in  $\{j, k\}$  and  $\{l, m\}$ , as

$$\hat{f}_{ijklm} = -\frac{1}{2} \hat{f} (e_{ilk} \delta_{jm} + e_{imk} \delta_{jl} + e_{ilj} \delta_{km} + e_{imj} \delta_{kl}) \quad (25)$$

so  $\hat{f}_{ijklm} \neq \hat{f}_{ilmjk}$  therefore this model does not have surface energy in the sense explained in this section.

#### 4. Chiral behaviour

Discussing the more general theory of elasticity with microstructure, Mindlin (1964) mentions that for centrosymmetric, isotropic materials the material parameters that are odd-rank tensors must be zero, and then implicitly uses the same result for gradient elasticity. It is common however, in the literature, to omit the reference to centrosymmetry when discussing the reduction from the linear to the isotropic case.

To obtain the form III expressions for a centrosymmetric isotropic material, however, isotropic odd-rank material parameter pseudo-tensors are indeed used. This leads to the presence of the  $\bar{f}$  parameter in equation (15), which is derived from  $\bar{f}_{ijklm}$  (while  $\bar{g}_{ijklm}$  vanishes anyway). The contribution of the even-rank tensor  $\bar{b}_{ijkl}$ , on the other hand, must be zero. This fact is however easily explained by considering the physical requirements for  $\bar{W}$ .

The value of the potential energy density  $\bar{W}$  should not depend on the choice of either a right-handed or left-handed coordinate system, therefore it must be a scalar and not a pseudo-scalar. The same requirement then applies to the terms in the sum defining

$\bar{W}$ , which must be themselves scalars. This does not mean that pseudo-tensorial quantities cannot appear in the expression of  $\bar{W}$ , indeed in form III the kinematic quantity  $\bar{\kappa}_{ij}$  is itself a pseudo-tensor. Pseudo-tensors must however be combined in such ways so as to make  $\bar{W}$  a scalar. For the linear case, this means that in equation (10)  $\bar{c}_{ijkl}$ ,  $\bar{d}_{ijkl}$ ,  $\bar{a}_{ijklmn}$  and  $\bar{g}_{ijklm}$  must be tensors while  $\bar{b}_{ijkl}$  and  $\bar{f}_{ijklm}$  must be pseudo-tensors. For the isotropic case, all material parameters in equation (15) must be scalars except for  $\bar{b}$  which must be pseudo-scalar.

As a pseudo-scalar,  $\bar{b}$  is a material parameter that discriminates between “right-hand” and “left-hand” deformations. Therefore, the presence of  $\bar{b}$  (or, alternatively,  $\hat{f}$  for mode II) introduces chirality in the behaviour of an isotropic linear gradient elastic material. It is thus seen that chirality is introduced not by the presence of deformation-type pseudo-tensors in the expression for the potential energy density, but by the presence of material parameters that are pseudo-tensors.

As clearly seen in the form III expression (15), chirality contributes to the potential energy density  $\bar{W}$  only if the rotation gradient  $\bar{\kappa}_{ij}$  is non-zero. Chirality in isotropic linear gradient elasticity is therefore only present in three-dimensional strain conditions, in which case the material can be seen as discriminating between right-hand and left-hand torsion. This can be easily seen in the examples presented in section 6.

## 5. Stress-strain relations, equilibrium equation and numerical implementation

### 5.1. Stress-strain relations and equilibrium equation

Considering the case of form II isotropic linear gradient elasticity, the stresses and double-stresses are easily derived from equation (14) as

$$\tau_{ij} = \lambda \delta_{ij} \epsilon_{pp} + 2\mu \epsilon_{ij} + \hat{f}(e_{pqi} \hat{\kappa}_{pqj} + e_{pqj} \hat{\kappa}_{pqi}) \quad (26)$$

$$\begin{aligned} \hat{\mu}_{ijk} = & \frac{1}{2} \hat{a}_1 (\delta_{ij} \hat{\kappa}_{kpp} + 2\delta_{jk} \hat{\kappa}_{ppi} + \delta_{ik} \hat{\kappa}_{jpp}) + 2\hat{a}_2 \delta_{jk} \hat{\kappa}_{ipp} \\ & + \hat{a}_3 (\delta_{ij} \hat{\kappa}_{ppk} + \delta_{ik} \hat{\kappa}_{ppj}) + 2\hat{a}_4 \hat{\kappa}_{ijk} \\ & + \hat{a}_5 (\hat{\kappa}_{kji} + \hat{\kappa}_{jki}) + \hat{f}(e_{ikp} \epsilon_{jip} + e_{ijp} \epsilon_{kjp}) \end{aligned} \quad (27)$$

where the terms containing  $\hat{f}$  are those related to the chiral behaviour. These additional terms introduce dependence of the stresses on the strain gradients and of the double

stresses on the strains.

The equilibrium equation in terms of stresses and double stresses does not depend on the constitutive model used and is therefore the same as given by [Mindlin \(1964\)](#),

$$(\tau_{jk} - \hat{\mu}_{ijk,i})_{,j} + F_k = 0 \quad (28)$$

where  $F_k$  are body forces. Substituting the stress-strain equations (26) and (27) into equation (28) and using the definitions (5) yields the equilibrium equation in terms of displacements

$$\begin{aligned} & (\lambda + 2\mu)(u_{p,pk} - l_1^2 u_{p,psk}) \\ & - \mu((u_{p,pk} - u_{k,pp}) - l_2^2(u_{p,psk} - u_{k,pps})) \\ & + \hat{f} e_{pqk} u_{q,ps} + F_k = 0 \end{aligned} \quad (29)$$

where the lengths  $l_1$  and  $l_2$  are given by

$$l_1^2 = \frac{2(\hat{a}_1 + \hat{a}_2 + \hat{a}_3 + \hat{a}_4 + \hat{a}_5)}{\lambda + 2\mu}, \quad l_2^2 = \frac{\hat{a}_3 + 2\hat{a}_4 + \hat{a}_5}{2\mu} \quad (30)$$

Considering for simplicity Cartesian coordinates, we note that for plane strain conditions ( $u_z = 0, \partial/\partial z = 0$ ) the equilibrium equation (29) in the  $x$  and  $y$  directions do not include  $\hat{f}$  and coincide with those for the non-chiral case. The equilibrium equation in the  $z$  direction, however, does not vanish but becomes

$$\hat{f} \left( \frac{\partial^2}{\partial x^2} + \frac{\partial^2}{\partial y^2} \right) \left( \frac{\partial u_y}{\partial x} - \frac{\partial u_x}{\partial y} \right) = 0 \quad (31)$$

This means that a problem that has a plane strain solution for  $\hat{f} = 0$  may not have such a solution for  $\hat{f} \neq 0$ . However, if the problem does have a plane strain solution for  $\hat{f} \neq 0$ , then this solution does not depend on  $\hat{f}$  (the corresponding term in  $\hat{W}$  is identically zero) and therefore does not exhibit chiral behaviour.

## 5.2. Numerical implementation

In the finite-element method it is useful to express the stress-strain relation in a matrix form. In gradient elasticity this is efficiently done by introducing a “generic stress” vector  $\check{\tau}$  that includes both stresses and double-stresses and a “generic strain”

vector  $\check{\epsilon}$  that includes both strains and strain gradients ([Papanicolopoulos et al., 2010](#)) defined so that

$$\check{\epsilon}^T \check{\tau} = \tau_{ij} \epsilon_{ij} + \hat{\mu}_{ijk} \hat{k}_{ijk} \quad (32)$$

The ordering of the components in  $\check{\epsilon}$  and  $\check{\tau}$  can be selected arbitrarily, as long as it is the same in both vectors. A convenient, though at first sight counterintuitive, form of these vectors is

$$\begin{aligned} \check{\epsilon}^T = \{ & \epsilon_{11} \ \epsilon_{22} \ \epsilon_{33} \ 2\hat{k}_{123} \ 2\hat{k}_{231} \ 2\hat{k}_{312} \\ & \hat{k}_{333} \ \hat{k}_{311} \ \hat{k}_{322} \ 2\hat{k}_{131} \ 2\hat{k}_{223} \ 2\epsilon_{12} \\ & \hat{k}_{111} \ \hat{k}_{122} \ \hat{k}_{133} \ 2\hat{k}_{212} \ 2\hat{k}_{331} \ 2\epsilon_{23} \\ & \hat{k}_{222} \ \hat{k}_{233} \ \hat{k}_{211} \ 2\hat{k}_{323} \ 2\hat{k}_{112} \ 2\epsilon_{31} \} \end{aligned} \quad (33)$$

$$\begin{aligned} \check{\tau}^T = \{ & \tau_{11} \ \tau_{22} \ \tau_{33} \ \hat{\mu}_{123} \ \hat{\mu}_{231} \ \hat{\mu}_{312} \\ & \hat{\mu}_{333} \ \hat{\mu}_{311} \ \hat{\mu}_{322} \ \hat{\mu}_{131} \ \hat{\mu}_{223} \ \tau_{12} \\ & \hat{\mu}_{111} \ \hat{\mu}_{122} \ \hat{\mu}_{133} \ \hat{\mu}_{212} \ \hat{\mu}_{331} \ \tau_{23} \\ & \hat{\mu}_{222} \ \hat{\mu}_{233} \ \hat{\mu}_{211} \ \hat{\mu}_{323} \ \hat{\mu}_{112} \ \tau_{31} \} \end{aligned} \quad (34)$$

The stress-strain relation can be written in the simple matrix form

$$\check{\tau} = \mathbf{D} \check{\epsilon} \quad (35)$$

For the specific form of  $\check{\epsilon}$  and  $\check{\tau}$  given in equations (33) and (34), the matrix  $\mathbf{D}$  has the block-diagonal form

$$\mathbf{D} = \begin{bmatrix} \mathbf{D}_{(1)} & \cdot & \cdot & \cdot \\ \cdot & \mathbf{D}_{(2)} & \cdot & \cdot \\ \cdot & \cdot & \mathbf{D}_{(2)} & \cdot \\ \cdot & \cdot & \cdot & \mathbf{D}_{(2)} \end{bmatrix} \quad (36)$$

where the matrices  $\mathbf{D}_{(1)}$  and  $\mathbf{D}_{(2)}$  are given by

$$\mathbf{D}_{(1)} = \begin{bmatrix} \lambda + 2\mu & \lambda & \lambda & \cdot & \hat{f} & -\hat{f} \\ \lambda & \lambda + 2\mu & \lambda & -\hat{f} & \cdot & \hat{f} \\ \lambda & \lambda & \lambda + 2\mu & \hat{f} & -\hat{f} & \cdot \\ \cdot & -\hat{f} & \hat{f} & \hat{a}_4 & \frac{1}{2}\hat{a}_5 & \frac{1}{2}\hat{a}_5 \\ \hat{f} & \cdot & -\hat{f} & \frac{1}{2}\hat{a}_5 & \hat{a}_4 & \frac{1}{2}\hat{a}_5 \\ -\hat{f} & \hat{f} & \cdot & \frac{1}{2}\hat{a}_5 & \frac{1}{2}\hat{a}_5 & \hat{a}_4 \end{bmatrix} \quad (37)$$

$$\mathbf{D}_{(2)} = \begin{bmatrix} 2(\hat{a}_1 + \hat{a}_2 + \hat{a}_3 + \hat{a}_4 + \hat{a}_5) & \hat{a}_1 + 2\hat{a}_2 & \hat{a}_1 + 2\hat{a}_2 & \frac{1}{2}\hat{a}_1 + \hat{a}_3 & \frac{1}{2}\hat{a}_1 + \hat{a}_3 & \cdot \\ \hat{a}_1 + 2\hat{a}_2 & 2(\hat{a}_2 + \hat{a}_4) & 2\hat{a}_2 & \frac{1}{2}\hat{a}_1 + \hat{a}_5 & \frac{1}{2}\hat{a}_3 & \hat{f} \\ \hat{a}_1 + 2\hat{a}_2 & 2\hat{a}_2 & 2(\hat{a}_2 + \hat{a}_4) & \frac{1}{2}\hat{a}_3 & \frac{1}{2}\hat{a}_1 + \hat{a}_5 & -\hat{f} \\ \frac{1}{2}\hat{a}_1 + \hat{a}_3 & \frac{1}{2}\hat{a}_1 + \hat{a}_5 & \frac{1}{2}\hat{a}_3 & \frac{1}{2}\hat{a}_3 + \hat{a}_4 + \frac{1}{2}\hat{a}_5 & \frac{1}{2}\hat{a}_3 & -\frac{1}{2}\hat{f} \\ \frac{1}{2}\hat{a}_1 + \hat{a}_3 & \frac{1}{2}\hat{a}_3 & \frac{1}{2}\hat{a}_1 + \hat{a}_5 & \frac{1}{2}\hat{a}_3 & \frac{1}{2}\hat{a}_3 + \hat{a}_4 + \frac{1}{2}\hat{a}_5 & \frac{1}{2}\hat{f} \\ \cdot & \hat{f} & -\hat{f} & -\frac{1}{2}\hat{f} & \frac{1}{2}\hat{f} & \mu \end{bmatrix} \quad (38)$$

Besides allowing for simpler finite-element computations, the form of the  $\mathbf{D}$  matrix presented here also provides a clear representation of which components of the static quantities are related to which components of the kinematic quantities and how these relations are affected by the introduction of chiral behaviour.

Note that many different formulations have been proposed in the literature for the numerical solution of gradient elasticity problems (though in most cases only two-dimensional problems are considered). In the case of  $C^1$  finite elements (Zervos et al., 2009) and  $C^1$  natural elements (Fischer et al., 2010) chirality is easily introduced by using directly the constitutive matrix  $\mathbf{D}$  presented here. The same applies to mixed elements with Lagrange multipliers (Matsushima et al., 2002), where equation (36) gives a submatrix of the total constitutive matrix.

In other cases, however, such as when using penalty methods (Zervos, 2008), implicit gradient models (Askes and Gutiérrez, 2006) or the boundary element method (Tsepoura et al., 2003), additional calculations must be carried out to properly introduce the chiral behaviour.

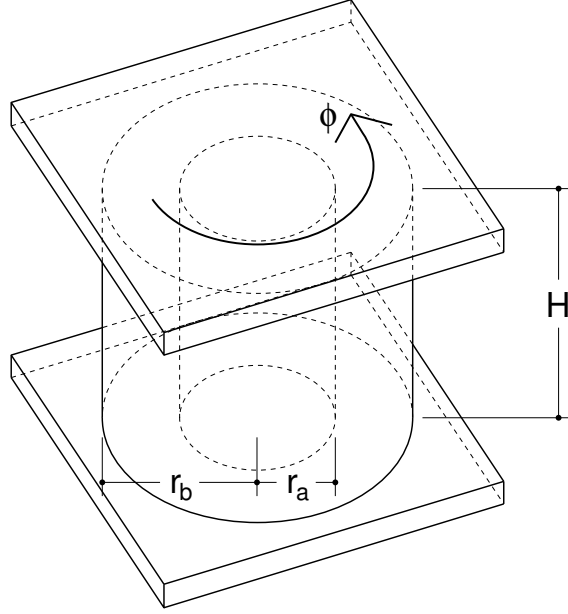


Figure 1: Torsion of a hollow cylinder.

## 6. Example problems

This section presents two simple examples showing the effect of chirality in the mechanical behaviour of an isotropic linear gradient elastic material.

### 6.1. Torsion of a hollow cylinder

#### 6.1.1. Problem description and analytical solution

Consider a cylinder of height  $H$  internal radius  $r_a$  and external radius  $r_b$  (see figure 1). The cylinder is subjected to torsion by two rigid plates: the lower one is kept fixed ( $u_\theta = u_z = 0$  for  $z = 0$ ) while the upper one is rotated by an angle  $\varphi$  around the  $z$  axis ( $u_\theta = \varphi r$ ,  $u_z = 0$  for  $z = H$ ). To further simplify the solution, the additional boundary condition  $\partial u_r / \partial z = 0$  is applied at both  $z = 0$  and  $z = H$  (while the displacement  $u_r$  is unconstrained).

The analytical solution, presented in detail in [Appendix A](#), gives the following expressions for the displacement field

$$u_r = \frac{\hat{f}\varphi r}{2(\lambda + \mu)H}, \quad u_\theta = \frac{\varphi r z}{H}, \quad u_z = 0 \quad (39)$$



For  $\hat{f} = 0$  we obtain  $u_r = 0$  and the gradient elastic solution for the displacements coincides with the solution of classical elasticity. If  $\hat{f} \neq 0$ , however, then  $u_r \neq 0$ , therefore torsion produces radial deformation. Moreover, the sign of  $u_r$  depends on the sign of the product  $\hat{f}\varphi$ . If  $\hat{f}\varphi > 0$ , i.e.  $\varphi$  has the same sign as  $\hat{f}$ , then torsion produces dilation in the radial direction, otherwise it produces contraction. The material therefore exhibits chirality, since the presence of the  $\hat{f}$  material parameter discriminates between the two directions of torsion.

As an indication of the relative magnitude of the radial and tangential displacement, we consider here the ratio of the maximum radial displacement (occurring on the exterior surface of the cylinder) over the maximum tangential displacement (occurring on the top exterior edge). From equations (39) and (22)

$$\frac{u_r^{\max}}{u_\theta^{\max}} = \frac{|\hat{f}|}{2(\lambda + \mu)H} < \frac{\sqrt{\mu(2\hat{a}_4 - \hat{a}_5)}}{2\sqrt{3}(\lambda + \mu)H} \quad (40)$$

In the usually employed case where  $\hat{a}_1 = \hat{a}_3 = \hat{a}_5 = 0$  and  $l_1 = l_2 = l$ , the above relation yields

$$\frac{u_r^{\max}}{u_\theta^{\max}} < \frac{1 - 2\nu}{\sqrt{6}} \frac{l}{H} \quad (41)$$

where  $\nu$  is Poisson's ratio. Since  $l$  is considered to be a length related to microstructure that is quite smaller than the size of the specimen (given here by the height  $H$ ), the above relation shows that  $u_r^{\max}$  will be also quite smaller than  $u_\theta^{\max}$ .

### 6.1.2. Numerical solution

The problem presented in section 6.1.1 is solved here using the finite-element method. We use a three-dimensional  $C^1$  formulation with tri-cubic Hermite hexahedra (Papanicolopoulos et al., 2009), which has been shown to provide sufficient accuracy even when using a small number of elements. As mentioned in section 5, chirality is conveniently introduced in this formulation just by adding in  $\mathbf{D}$  the terms including the  $\hat{f}$  parameter, without the need for any additional calculation.

The material parameters used are  $\lambda = 7000$ ,  $\mu = 3000$ ,  $l_1 = l_2 = 0.001$ ,  $a_1 = a_3 = a_5 = 0$ ,  $a_2 = \lambda l_1^2/2 = 0.0035$ ,  $a_4 = \mu l_2^2 = 0.003$  and  $\hat{f} = 2$ . The geometry and applied displacements are given by  $H = 0.02$ ,  $r_a = 0.02$ ,  $r_b = 0.04$  and  $\phi = \pm 0.002$ .

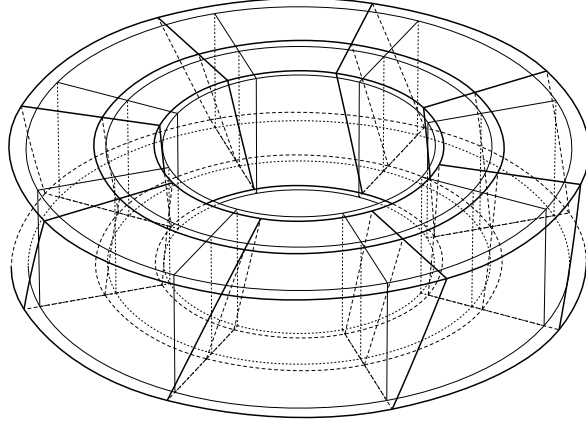


Figure 2: Finite element results for the torsion of a hollow cylinder, for  $\phi > 0$  and  $\hat{f} > 0$  (thin lines indicate the undeformed mesh).

The results are shown in figure 2 for  $\phi > 0$  and figure 3 for  $\phi < 0$ , in both cases for a coarse mesh with 16 elements. The displacements at the top exterior edge are calculated analytically as  $u_\theta = 8 \cdot 10^{-5}$  and  $u_r = 4 \cdot 10^{-7}$ , and are computed numerically with a relative error of less than 1%.

Following usual finite element practice, the displacements in figures 2 and 3 have been exaggerated. Note however that the scaling has been carried out in cylindrical coordinates (while the computations are obviously done in Cartesian coordinates), since scaling in Cartesian coordinates would introduce a non-physical change of the radii of the upper face. The use of scaling in cylindrical coordinates also allows for different scaling factors in the radial and tangential directions (6000 times and 100 times respectively in these examples) to make evident the change in radius due to chirality.

## 6.2. Mode III crack

The mode III crack in (non-chiral) linear gradient elasticity has been considered by different authors (e.g. [Vardoulakis et al., 1996](#); [Zhang et al., 1998](#); [Georgiadis, 2003](#)). Detailed numerical results are presented by [Papanicolopulos and Zervos \(2010\)](#).

Consider the body given in figure 4, with a zero-width crack subjected to mode III deformation. To allow for simpler computations, the body is considered to be infinitely long in the  $z$  direction, so that all fields depend only on  $x$  and  $y$ .

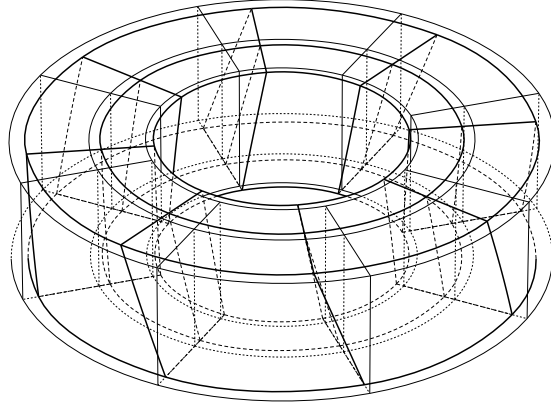


Figure 3: Finite element results for the torsion of a hollow cylinder, for  $\phi < 0$  and  $\hat{f} > 0$  (thin lines indicate the undeformed mesh).

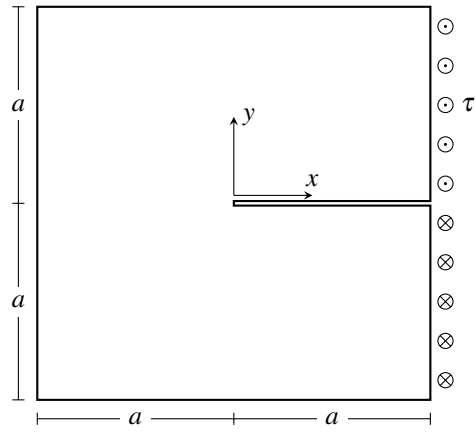


Figure 4: A zero-width crack under mode III deformation

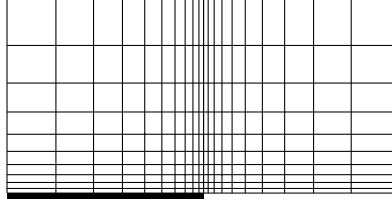


Figure 5: Mesh used for the mode III crack problem (symmetry/antisymmetry conditions applied along thick line)

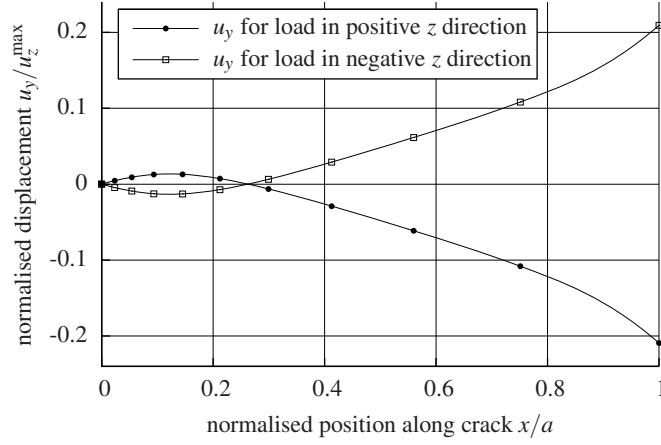


Figure 6: Mode III crack: crack opening displacement in  $y$  direction

The problem is solved numerically using a single layer of tri-cubic Hermite hexahedra, with the appropriate degrees of freedom set to zero to make the solution independent of  $z$ . The material parameters are the same as in the previous example, while  $a = 0.01$  and the applied load is  $\tau = \pm 3$ . Taking advantage of the symmetries and antisymmetries of the problem and imposing the appropriate boundary conditions, only the upper half of the body is discretised, using a non-uniform structured mesh of 200 elements, as shown in figure 5.

While in the classical and in the non-chiral gradient case the only non-zero displacement component is  $u_z(x, y)$ , the numerical results show that in the chiral case  $u_x(x, y)$  and  $u_y(x, y)$  are also non-zero. Indicatively, figure 6 shows the displacement in the  $y$  direction of the *upper* face of the crack (normalised by the  $u_z$  displacement of the

edge of the crack).

The mechanical response is chiral since reversing the load, and therefore the direction of torsion, changes the sign of the displacement  $u_y$  (which would be zero in the non-chiral case).

Note that the displacement  $u_y$  of the *lower* face of the crack (which is not discretised in this example) is equal and opposite to that of the upper face. As shown in figure 6, however, for both load directions one part of the upper face will have  $u_y < 0$ , with the respective part of the lower face having  $u_y > 0$ . The actual solution of the problem is therefore more complex, as it involves contact between the crack faces. This has actually been found to be the case also for different other mode III crack geometries.

## 7. Conclusions

While it is usual to consider only the centrosymmetric behaviour of gradient elastic solids, the theory of gradient elasticity is able to describe chiral behaviour even in the isotropic linear case. This paper shows how for isotropic materials this behaviour is represented by the introduction of a single additional material parameter, in contrast to the usually employed isotropic linear Cosserat elasticity which introduces three different additional parameters related to chirality.

Positive definiteness of the potential energy density imposes a bound on the absolute value of the additional parameter, which however can be either negative or positive. Indeed, it is shown that this parameter is a pseudo-scalar, and therefore its sign is actually dependent on the handedness of the coordinate system, without however affecting the overall material behaviour which remains independent of the coordinate system, and thus objective. As the chiral effect depends on the gradient of rotation, the sign of the additional parameter relative to the handedness of the coordinate system discriminates between left-handed and right-handed torsion. This is clearly shown using two example problems.

The applicability of the model presented in this paper to specific materials, for example carbon nanotubes as mentioned in the introduction or other materials exhibiting chirality, is a hypothesis which requires extensive experimental verification, as is

always the case in continuum modelling. Another important issue is linking the continuum chiral behaviour to specific properties of the discrete material microstructure. As this is actually a part of a much more general open problem, that concerns the whole of the gradient elastic behaviour and not only its chiral part, extensive additional research is needed in this direction.

### Acknowledgements

The research leading to these results has received funding from the European Research Council under the European Community's Seventh Framework Programme (FP7/2007–2013) / ERC grant agreement n° 228051 (MEDIGRA).

### Appendix A. Analytical solution of hollow cylinder torsion

To obtain an analytical solution to the problem of the torsion of a hollow cylinder, described in section 6, we assume the following general form of the solution for the displacements in cylindrical coordinates

$$u_r = A(r), \quad u_\theta = rB(z), \quad u_z = 0 \quad (\text{A.1})$$

Substituting into the equilibrium equation (29) yields the following differential equations

$$(\lambda + 2\mu)(1 - l_1^2 \nabla^2) \nabla^2 A(r) - \hat{f} r \frac{d^3 B(z)}{dz^3} = 0 \quad (\text{A.2})$$

$$\mu \left( 1 - l_2^2 \frac{d^2}{dz^2} \right) \frac{d^2}{dz^2} B(z) = 0 \quad (\text{A.3})$$

$$\hat{f} \frac{d^2}{dz^2} B(z) = 0 \quad (\text{A.4})$$

where the Laplacian in equation (A.2) is given by

$$\nabla^2 = \frac{d^2}{dr^2} + \frac{1}{r} \frac{d}{dr} - \frac{1}{r^2} \quad (\text{A.5})$$

For  $\hat{f} \neq 0$ , equation (A.4) together with the boundary conditions  $u_\theta = 0$  for  $z = 0$  and  $u_\theta = r\phi$  for  $z = H$  yield the solution  $u_z = r\phi z/H$ . This solution satisfies equation (A.3), while equation (A.2) yields

$$A(r) = C_1 r + C_2/r + C_3 I_1(r/l_1) + C_4 K_1(r/l_1) \quad (\text{A.6})$$

where  $I_1$  and  $K_1$  are the modified Bessel functions of the first and second kind respectively and of order one. Requiring that the tractions and double tractions on the internal and external faces of the hollow cylinder are all zero yields after extensive calculations

$$C_1 = \frac{1}{2} \frac{\hat{f}}{\lambda + \mu} \frac{\phi}{H}, \quad C_2 = C_3 = C_4 = 0 \quad (\text{A.7})$$

so that finally the solution of the problem is

$$u_r = \frac{\hat{f}\varphi r}{2(\lambda + \mu)H}, \quad u_\theta = \frac{\varphi r z}{H}, \quad u_z = 0 \quad (\text{A.8})$$

The non-zero tractions and double tractions on the top face are

$$\hat{P}_\theta = \frac{\mu\phi r}{H}, \quad \hat{P}_z = \frac{4\lambda + 3\mu}{\lambda + \mu} \frac{\hat{f}\phi}{H}, \quad \hat{R}_r = \frac{\hat{f}\phi r}{2H} \quad (\text{A.9})$$

The non-zero edge tractions on the top exterior edge are

$$\hat{E}_\theta = \left( 2\hat{a}_4 - \hat{a}_5 - \frac{\hat{f}^2}{\lambda + \mu} \right) \frac{\phi}{2H}, \quad \hat{E}_z = -\frac{\hat{f}\phi r}{2H} \quad (\text{A.10})$$

while on the top interior edge the edge tractions are equal and opposite. Similar expressions hold for the bottom face and bottom edges, with all signs reversed except for  $\hat{R}_r$ .

The tractions  $\hat{P}_\theta$  and  $\hat{E}_\theta$  are actually reactions to the imposed tangential displacement, while  $\hat{P}_z$  and  $\hat{E}_z$  are reactions to the imposed zero displacement in the  $z$  direction. Since for  $\hat{f} \neq 0$  the double traction  $\hat{R}_r$  is not zero, it is necessary to impose the additional boundary condition  $\partial u_r / \partial z = 0$  on the top and bottom faces in order to obtain the solution (A.8).

## References

- Agiasofitou, E.K., Lazar, M., 2009. Conservation and balance laws in linear elasticity of grade three. *J. Elast.* 94, 69–85.
- Askes, H., Gutiérrez, M.A., 2006. Implicit gradient elasticity. *Int. J. Numer. Methods Eng.* 67, 400–416.

- Auffray, N., Bouchet, R., Bréchet, Y., 2009. Derivation of anisotropic matrix for bi-dimensional strain-gradient elasticity behavior. *Int. J. Solids Struct.* 46, 440–454.
- Borisenko, A.I., Tarapov, I.E., 1979. Vector and tensor analysis with applications. Dover Publications, New York.
- Boyle, L.L., Matthews, P.S.C., 1971. The isotropic invariants of fifth-rank Cartesian tensors. *Int. J. Quantum Chem.* 5, 381–386.
- Casal, P., 1961. La capillarité interne. *Cahier du Groupe Français d'Etudes de Rheologie*, C.N.R.S. VI, 31–37.
- Cintas, P., 2007. Tracing the origins and evolution of chirality and handedness in chemical language. *Angew. Chem. Int. Ed.* 46, 4016–4024.
- Cosserat, E., Cosserat, F., 1909. *Théorie des Corps Déformables*. A. Hermann, Paris.
- Duan, W., Wang, Q., Liew, K., He, X., 2007. Molecular mechanics modeling of carbon nanotube fracture. *Carbon* 45, 1769 – 1776.
- Eringen, A.C., 1966. Linear theory of micropolar elasticity. *J. Math. Mech.* 15, 909–923.
- Fischer, P., Mergheim, J., Steinmann, P., 2010. On the C1 continuous discretization of non-linear gradient elasticity: A comparison of NEM and FEM based on Bernstein-Bézier patches. *Int. J. Numer. Methods Eng.* 82, 1282–1307.
- Fraldi, M., Cowin, S., 2002. Chirality in the torsion of cylinders with trigonal symmetry. *J. Elast.* 69, 121–148.
- Georgiadis, H.G., 2003. The mode III crack problem in microstructured solids governed by dipolar gradient elasticity: Static and dynamic analysis. *J. Appl. Mech.* 70, 517–530.
- Georgiadis, H.G., Grentzelou, C.G., 2006. Energy theorems and the  $J$ -integral in dipolar gradient elasticity. *Int. J. Solids Struct.* 43, 5690–5712.



- Giannakopoulos, A.E., Amanatidou, E., Aravas, N., 2006. A reciprocity theorem in linear gradient elasticity and the corresponding Saint-Venant principle. *Int. J. Solids Struct.* 43, 3875–3894.
- Lord Kelvin, 1904. *Baltimore lectures on molecular dynamics and the wave theory of light*. C. J. Clay and Sons, London.
- Lakes, R., 2001. Elastic and viscoelastic behavior of chiral materials. *Int. J. Mech. Sci.* 43, 1579 – 1589.
- Lakes, R.S., Benedict, R.L., 1982. Noncentrosymmetry in micropolar elasticity. *Int. J. Eng. Sci.* 20, 1161 – 1167.
- Maranganti, R., Sharma, P., 2007. A novel atomistic approach to determine strain-gradient elasticity constants: Tabulation and comparison for various metals, semiconductors, silica, polymers and the (ir) relevance for nanotechnologies. *J. Mech. Phys. Solids* 55, 1823–1852.
- Matsushima, T., Chambon, R., Caillerie, D., 2002. Large strain finite element analysis of a local second gradient model: application to localization. *Int. J. Numer. Methods Eng.* 54, 499–521.
- Mindlin, R.D., 1964. Micro-structure in linear elasticity. *Arch. Ration. Mech. Anal.* 16, 51–78.
- Mindlin, R.D., Eshel, N.N., 1968. On first strain-gradient theories in linear elasticity. *Int. J. Solids Struct.* 4, 109–124.
- Mislow, K., 1999. Molecular chirality, in: Denmark, S.E. (Ed.), *Topics in Stereochemistry*. John Wiley & Sons. volume 22. chapter 1, pp. 1–82.
- Natroshevili, D., Stratis, I.G., 2006. Mathematical problems of the theory of elasticity of chiral materials for Lipschitz domains. *Math. Methods Appl. Sci.* 29, 445–478.
- Papanicolopoulos, S.A., 2008. Analytical and numerical solutions in boundary value problems of materials with microstructure. Ph.D. thesis. National Technical University of Athens.

- Papanicolopoulos, S.A., Zervos, A., 2010. Numerical solution of crack problems in gradient elasticity. *Eng. Comp. Mech.* 163, 73–82.
- Papanicolopoulos, S.A., Zervos, A., Vardoulakis, I., 2009. A three dimensional  $C^1$  finite element for gradient elasticity. *Int. J. Numer. Methods Eng.* 77, 1396–1415.
- Papanicolopoulos, S.A., Zervos, A., Vardoulakis, I., 2010. Discretization of gradient elasticity problems using  $C^1$  finite elements, in: Maugin, G.A., Metrikine, A.V. (Eds.), *Mechanics of Generalized Continua*. Springer, New York. volume 21 of *Advances in Mechanics and Mathematics*. chapter 28, pp. 269–277.
- Temple, G., 2004. *Cartesian tensors: An introduction*. Dover Publications, New York.
- Toupin, R.A., 1962. Elastic materials with couple stresses. *Arch. Ration. Mech. Anal.* 11, 385–414.
- Tsepoura, K.G., Tsinopoulos, S.V., Polyzos, D., Beskos, D.E., 2003. A boundary element method for solving 2-D and 3-D static gradient elastic problems: Part II: Numerical implementation. *Comput. Methods Appl. Mech. Eng.* 192, 2875–2907.
- Vardoulakis, I., Exadaktylos, G., Aifantis, E., 1996. Gradient elasticity with surface energy: Mode III crack problem. *Int. J. Solids Struct.* 33, 4531–4559.
- Wang, L., Hu, H., 2005. Flexural wave propagation in single-walled carbon nanotubes. *Phys. Rev. B* 71, 195412.
- Wang, Q., Wang, C.M., 2007. The constitutive relation and small scale parameter of nonlocal continuum mechanics for modelling carbon nanotubes. *Nanotechnology* 18, 075702.
- Zervos, A., 2008. Finite elements for elasticity with microstructure and gradient elasticity. *Int. J. Numer. Methods Eng.* 73, 564–595.
- Zervos, A., Papanicolopoulos, S.A., Vardoulakis, I., 2009. Two finite element discretizations for gradient elasticity. *J. Eng. Mech.-ASCE* 135, 203–213.

- Zhang, L., Huang, Y., Chen, J.Y., Hwang, K.C., 1998. The mode III full-field solution in elastic materials with strain gradient effects. *Int. J. Fract.* 92, 325–348.
- Zhang, Y., Wang, C., Xiang, Y., 2010. A molecular dynamics investigation of the torsional responses of defective single-walled carbon nanotubes. *Carbon* 48, 4100–4108.
- Zhang, Y.Q., Liu, G.R., Wang, J.S., 2004. Small-scale effects on buckling of multi-walled carbon nanotubes under axial compression. *Phys. Rev. B* 70, 205430.